

Regional Features of Interannual Variations in Water Temperature in the Subarctic Pacific

I. D. Rostov^{a*} and E. V. Dmitrieva^a

^a*Il'ichev Pacific Oceanological Institute, Far Eastern Branch, Russian Academy of Sciences,
ul. Baltiiskaya 43, Vladivostok, 690041 Russia*

**e-mail: rostov@poi.dvo.ru*

Received June 16, 2020

Revised June 16, 2020

Accepted October 6, 2020

Abstract—Based on the NOAA climate datasets, trends, regional features, and possible causal relationships of interannual variations in water temperature on the surface (SST) and in the upper 750-meter layer of the subarctic Pacific with variations in the fields of air temperature, air pressure, wind, and climate indices over the past four decades are identified. The results revealed a degree of heterogeneity of the study region response to the ongoing global climate change, identified isolated areas, and quantified the warming rate in these areas. It is shown that in the west of the region, the SST trends are much higher than in the east, and in the warm season, they are about twice higher than in the cold season. Changes in water temperature and heat content anomalies in the water column of different regions are extremely uneven. The phases of alternating warm and cold periods are consistent with trends in the characteristics of the atmospheric centers of action, climate indices, and different climatic parameters.

DOI: 10.3103/S1068373921020059

Keywords: Pacific Ocean, subarctic zone, climate change, water temperature, heat content, climate indices, trends, correlation, regional features

1. INTRODUCTION

Surface temperature and heat content of the ocean are among the seven major indicators of the climate state; even slow climate changes in large areas have long-term and large-scale consequences, that affect various economic and environmental spheres [2, 18]. The results of numerous studies indicate the ongoing global climate warming with significant spatiotemporal heterogeneity [5]. On the global scale, the greatest ocean temperature rise occurs near the surface and, according to the authors' estimates based on data from <https://www.esrl.noaa.gov/psd/>, average annual sea surface temperature (SST) in the subarctic Pacific (north of 40° N) during 1982–2019 had been increasing by ~0.2° C per decade and rose by 0.7° C over the whole analyzed period. In these years, the global warming was manifested in the SST rise in the Eastern Arctic seas: in the East Siberian, Chukchi, Laptev, and Kara seas by 2.6, 2.3, 1.3, and 2.4° C, respectively [12]. This is generally higher than the respective estimates for the marginal seas in the Western Pacific: the SST rise in the Okhotsk, Japan, Yellow (East China), and South China seas was 1.6, 1.2, 0.8, and 0.4° C, respectively [13].

Unlike SST, the ocean heat content increases more steadily, with less pronounced interannual fluctuations [27]. At the same time, more than 90% of the global increase in the heat content of ocean water is observed in the upper-kilometer layer. The value of heat content has been growing since the middle of the 20th century and has been record high in the recent years [18, 21, 27]. During the 40-year period from 1971 to 2010, more than 60% of the pure energy growth in the climate system was observed in the upper ocean layer (0–700 m). About 30% was registered at the depth of >700 m, that is much greater than the depth of penetration of seasonal fluctuations; therefore, they should be interpreted as climatic interdecadal ones [1]. In the layer of 0–700 m, the heat content in 2003–2010 was increasing more slowly than in 1993–2002

[18]: this is an effect of heat redistribution between separate layers of the water column and different parts of the World Ocean by means of horizontal advection. The sign and value of trends in SST and heat content of individual layers in different parts of the ocean can differ much from global trends.

The objective of the present paper is to refine tendencies and spatial features of interannual variations in SST and water temperature of the upper 750-meter layer in the subarctic Pacific [17, 26], as well as the analysis of their possible casual relationships with large-scale and regional processes in the ocean and atmosphere in the past four decades. A specific feature of the subarctic water structure is the presence of cold and warm intermediate layers typical of the North Pacific, including the Bering and Okhotsk seas. The large dimensions of the area and specific circulation features of the atmosphere and ocean form noticeable differences in weather and climate conditions in this area. They are mainly caused by the interaction of the three main seasonal atmospheric centers of action: the Aleutian Low, the North Pacific (Hawaii) High, and the winter Siberian High, which determine the wind field structure and the state of the upper ocean layer [2].

2. DATA AND METHODS

The following data were used to analyze interannual variations in water temperature T_w : NOAA OI SST V2 data of optimum interpolation of T_w on the ocean surface for 1982–2018 from <https://www.esrl.noaa.gov/psd/> [23], GODAS (Global Ocean Data Assimilation System) data on T_w and current velocity at different horizons [15] (<https://www.esrl.noaa.gov/psd/data/gridded/data.godas.html>) for 1980–2018, decadal data on regional climatology of T_w in the North Pacific [24] (https://www.nodc.noaa.gov/OC5/regional_climate/nnp-climate/), and information from the climate atlas for the North Pacific seas [22].

Data on surface air temperature T_a from the NCEP/NCAR Reanalysis-1 [19], on air pressure, wind, heat fluxes on the ocean surface, the series of climate (circulation) indices in common abbreviations [9, 13] (PDO, AMO, SOI, NPI, WP, PNA, EP/NP) were also used. The listed data were taken from <https://www.esrl.noaa.gov/psd/> (it was developed by NOAA/OAR/ESRL PSD, USA) and from the NOAA/NCEI/CPC websites <https://www.nodc.noaa.gov/> and <https://www.cpc.ncep.noaa.gov/>.

The comparability of quantitative estimates with the results obtained for the similar period for other geographic regions [12, 13] was provided by the calculation of statistical characteristics (mean values, variance, anomalies, correlation coefficients, trends for different seasons), the decomposition of fields into principal components of empirical orthogonal functions (EOFs). The cluster analysis by three principal components was used for the zoning [13]. Taking into account the duration of summer and winter monsoons in the Northwest Pacific and intraannual variations in T_a and SST, the conditionally warm (June–September) and conditionally cold (November–March) seasons were distinguished. The trends were estimated for the average annual and seasonal values of parameters and their anomalies. The anomalies were defined as a deviation from the mean over all years of the 30-year period of 1984–2013. The values of integral heat content Q [7] in different layers from the surface to the depth of 750 m, its anomalies and wind stress curl were also calculated [6].

3. RESULTS AND DISCUSSION

3.1. Features of Spatial and Interannual Variability of Sea Surface Temperature

Six relatively isolated regions were distinguished in the subarctic Pacific using SST data: the western part of the Bering Sea (WBS), Alaskan-Aleutian (AA), western subarctic (WSA), transition zone (TZ), eastern subarctic (ESA), and coastal (CO) ones; their location is shown in Fig. 1a. The area of the Sea of Okhotsk was not included to this scheme, as it has already been considered before [13]. The position of the distinguished regions is generally consistent with natural physiographic zones of the subarctic region and with the schemes of spatial features of structural and circulation characteristics of its water [17, 26].

The SST field is characterized by the positive values of trends (b) in average annual values of temperature almost in the entire subarctic region, and the zones of maximum SST trends ($b = 0.3\text{--}0.4$ C/10 years) are observed in the northwest and southwest; between these zones, there is an area with minimum root-mean-square values of SST fluctuations (Figs. 1a and 1b). During the warm season, the SST trends are higher than in the cold season, when the negative values of b are observed on a significant area (Figs. 1c and 1d). These spatial features of interannual SST variations are expressed in the corresponding quantitative estimates presented in Table 1.

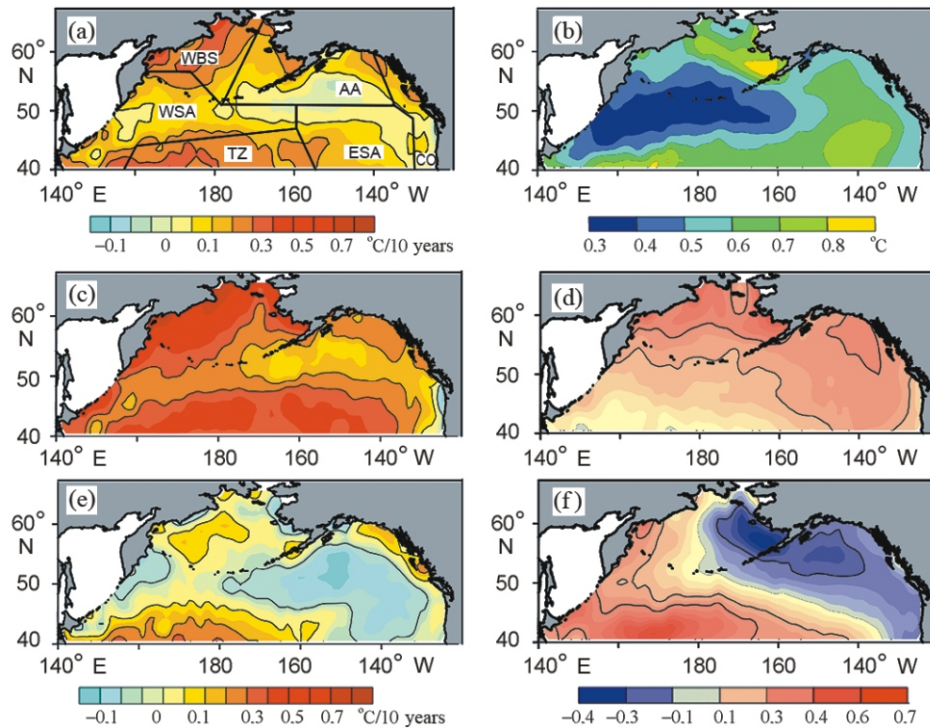


Fig. 1. The value of (a) trends and (b) root-mean-square values of average annual anomalies of SST, SST trends for (c) the warm and (e) cold seasons in 1982–2018, as well as the distribution of coefficients of (d) the first and (f) second EOF modes of interannual variations in the SST anomalies in the warm season. The location of the distinguished regions is shown in figure (a).

Table 1. The pattern and interannual trends in SST in the distinguished regions during 1982–2018

Region	b	tr	σ^2	D	b_{\max}	b_{warm}	b_{cold}	R
WBS	0.30	1.1	0.26	41	0.70 (August)	0.61	0.08	0.92
AA	0.11	0.4	0.28	5	0.24 (August)	0.22	0.00	0.97
WSA	0.16	0.6	0.09	33	0.42 (August)	0.31	0.06	0.91
TZ	0.25	0.9	0.27	28	0.56 (July)	0.42	0.15	0.94
ESA	0.13	0.5	0.34	5	0.39 (August)	0.30	0.00	0.95
CO	0.11	0.4	0.27	6	0.20 (November)	0.15	0.08	0.96
Entire sea area	0.18	0.7	0.12	31	0.70 (August)	0.34	0.06	0.97

Note: b is the coefficient of linear trend slope for average annual SST, $^{\circ}\text{C}$ per decade; tr is the trend over 37 years, $^{\circ}\text{C}$; σ^2 is variance; D is the trend contribution to total variance, %; b_{\max} is the maximum value of b (a month is given in brackets); b_{warm} , b_{cold} are the trend coefficients for the warm and cold seasons; R is the coefficient of correlation between average annual SST and T_a . Hereinafter, statistically significant estimates are bolded.

3.2. Pattern and Interannual Trends in Sea Surface Temperature in the Distinguished Regions during 1982–2018

The average annual SST rose by 0.4–1.1 $^{\circ}\text{C}$ in different areas of the subarctic region and by 0.7 $^{\circ}\text{C}$ in the whole region. The greatest statistically significant trends and their contribution to the total variance of average annual SST were registered in the WBS, WSA, and TZ regions, where the zone of the most active cyclogenesis has been located in the recent decades [4]. In the warm season, the SST trend is statistically significant in all regions, except for the coastal area of North America coast; in the cold season, this value is statistically insignificant in the whole subarctic Pacific. In the presence of the high correlation between the variations in T_a and SST (see Table 1), the mentioned peculiarities of changes in these climatic

parameters are consistent. The parts of the sea areas with the highest values of standard deviations of interannual variations in SST (> 0.6 C) are situated in the areas with maximum horizontal gradients of temperature and wind stress curl [17, 28]. In the field of wind stress curl, the values of τ in the cold season are on average twice higher than in the warm season.

The mentioned features of the spatiotemporal variability of SST result from the interaction of different-scale processes in the sea and the atmosphere. To reveal the most important components of this process, the EOFs of interannual variability of anomalies of SST, surface air temperature T_a , 500 hPa geopotential height (H_{500}), and wind stress curl were computed. The principal components of EOFs carry important information about the principal modes of large-scale interannual variability of these fields, and the time factors of the decomposition describe the interannual variations in the regional mean values of variance and trends. The first three modes C1–C3 of SST EOFs accumulate 74% of variance of interannual variations in the anomalies of average annual SST in the region.

The distribution of the coefficients C1 of SST EOFs in the warm season is represented by the positive values and characterizes in-phase SST variations (Fig. 1d) within the entire basin. At this time, the positive interannual trends are well pronounced both for SST (see Table 1) and for the first and second EOF principal components, and the highest values of C1 are registered in the WBS, AA, and WSA regions. The values of the contribution of the SST trend (see Table 1) and the first mode of SST decomposition to total variance are close. The distribution of C2 forms a dipole with the centers in the AA and TZ regions (Fig. 1f). In the warm season, the interannual variations in both modes highly correlate with air temperature fluctuations in the whole Northern Hemisphere ($R = 0.4–0.6$). In the cold season, when the transformation of the atmospheric circulation occurs, the correlation of spatiotemporal variations in SST decreases, and the trends in SST and SST EOF C1, C2 modes are not pronounced. The results of the correlation analysis indicate the influence of different atmospheric processes and variability of the main climatic parameters (air temperature, air pressure, and wind) on the formation of the structure of the distinguished SST EOF modes. For example, variations in H_{500} in the middle troposphere highly correlate with the state of the atmospheric centers of action, with changes in the respective climate indices, the characteristics of temperature and wind regimes and are most strongly manifested in the study region. The wind stress curl is one of the important quantitative characteristics of the spatial inhomogeneity of the wind field [6] and dynamic effect on the sea surface, including the vertical circulation, water sinking and lifting [3]. Unlike SST and H_{500} , the distribution of this parameter is substantially uneven and focal; due to this fact, the contribution of three principal EOF modes to total variance of τ in different seasons does not exceed 35–45%. Its peculiarity is a good agreement between the location of the zones with maximum values of trends b , standard deviations σ , and the C1 field of wind stress curl τ . At the same time, the positive values of τ correspond to the cyclonic wind stress curl and the negative values correspond to the anticyclonic one. In general for the region, the negative trends both in wind stress curl and distinguished EOF modes of this parameter were observed in the warm and cold seasons. As shown below, the interannual changes in water temperature in most of the distinguished regions are connected with the first SST EOF mode describing 40% of total variance for the field of interannual variations in the anomalies of average annual SST (Δv), as well as SST in the warm (W) and cold (C) seasons:

Region	WBS			AA			WSA			TZ			ESA			CO		
	Av	W	C	Av	W	C	Av	W	C	Av	W	C	Av	W	C	Av	W	C
C1	0.8	0.9	0.6	0.9	0.8	0.9	0.4	0.6	-0.4	-0.1	0.3	-0.7	0.8	0.8	0.6	0.9	0.8	0.8
C2	0.3	0.1	0.2	-0.3	-0.4	0.1	0.8	0.6	0.7	1.0	0.9	0.7	0.3	0.0	0.8	-0.1	-0.3	0.0
C3	0.5	0.3	0.4	0.1	0.0	0.1	0.3	0.1	0.5	0.0	-0.1	0.2	-0.5	-0.6	-0.2	0.0	-0.1	0.4

In each region, essential differences were observed in the amplitude and synchronicity of variations in the SST anomalies, which are especially noticeable when comparing the curves of T_w for the western and eastern sectors of the subarctic Pacific (Fig. 2). The integral curves of cumulative anomalies correspond to different phases of alternating warm and cold periods, and individual extremes on the curves of T_w emphasize a heterogeneous pattern of the warming in space and time. The phase of accumulation of positive SST anomalies is pronounced after 2003 in the western part of the subarctic Pacific (Figs. 2b, 2f, and 2h) and only in a decade in its eastern part.

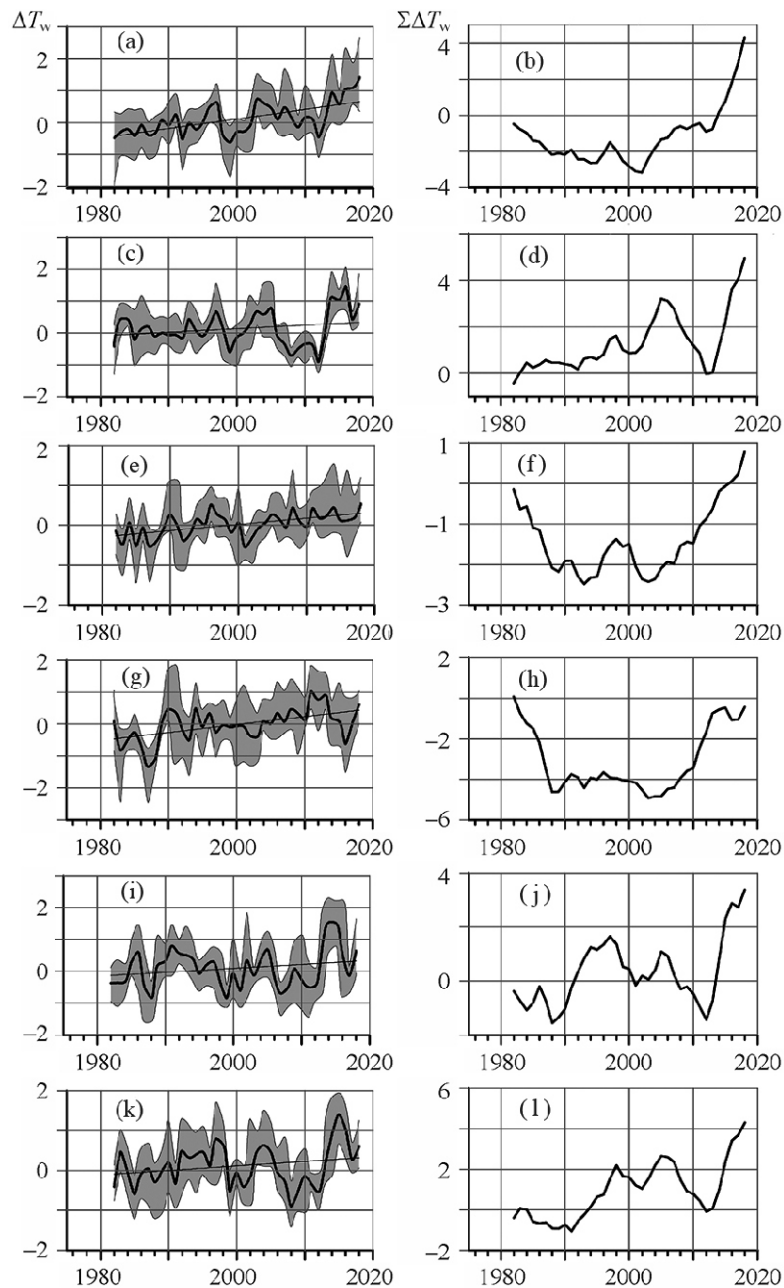


Fig. 2. The interannual variability of (a, c, e, g, i, k) the anomalies of average annual water temperature T_w and (b, d, f, h, j, l) cumulative anomalies $\Sigma\Delta T_w$ in the distinguished regions: (a, b) WBS; (c, d) AA; (e, f) WSA; (g, h) TZ; (i, j) ESA; (k, l) CO. In the figures, the left column shows the range of intraannual variations, the regional mean values, and the trend lines.

3.3. Variability of Temperature and Heat Content in the Surface and Intermediate Layers

Based on the GODAS data [15], the mean values of T_w and the anomalies of integral heat content [7] in different layers from the surface to the depth of 750 m were calculated. In the layer of 25–100 m, there are the maximum amplitudes of seasonal variations in T_w , and its base roughly corresponds to the position of the core of the cold intermediate layer of subarctic water structure. In the recent four decades, the value of the difference in maximum and minimum average annual values T_w at the base of the cold intermediate layer varied in different regions by 0.9–2.5 °C. The base of the second distinguished layer (100–250 m) corresponds to the depth of the active layer in the subarctic region. The value of the difference T_w in different regions decreases to 0.5–1.6 °C at the horizon of 250 m and to 0.2–1.3 °C in the subsurface layer at the depth of 500 m. In the intermediate layer below 500–600 m, the seasonal fluctuations damp [1].

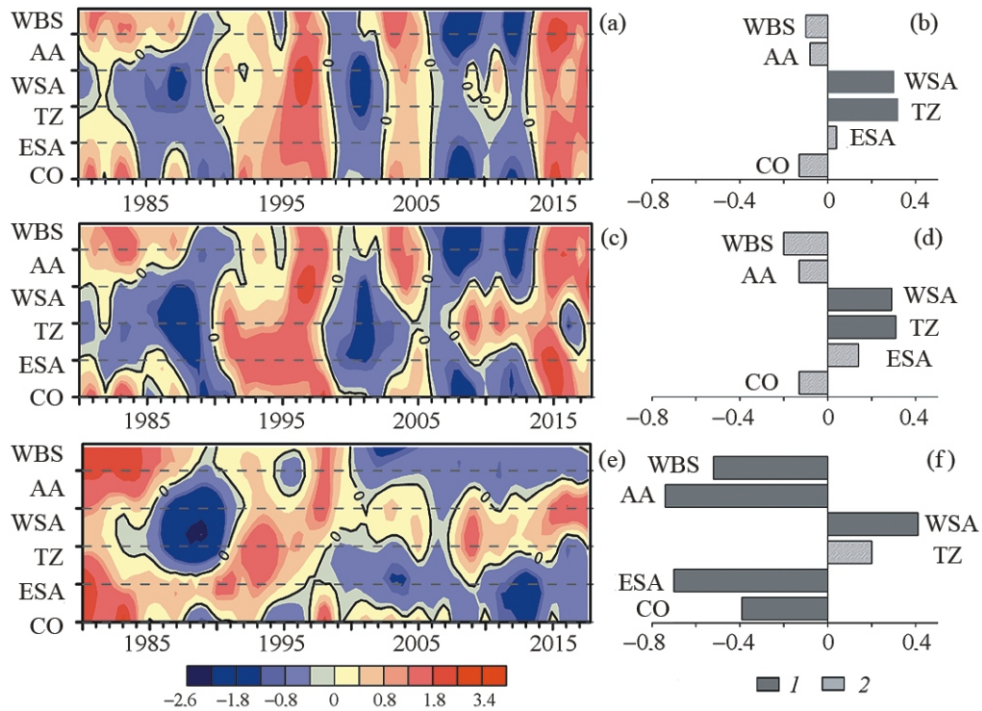


Fig. 3. (a, c, e) The interannual variations in the normalized anomalies of integral heat content and (b, d, f) their trends in different areas of the subarctic region in the layers of (a, b) 5–100, (c, d) 100–250, and (e, f) 250–750 m according to GODAS average annual data. (1) Statistically significant estimates of trends; (2) statistically insignificant estimates.

The positive trends in T_w and Q were observed in all analyzed layers in the WSA and TZ regions, and the negative trends were registered in the WBS, AA, and CO regions, which is mainly consistent with the results obtained from instrumental observations [1, 22, 24]; in the ESA region, the opposite trends are observed in the upper (to 250 m) and lower (250–750 m) layers of the water column (Fig. 3). Statistically significant negative trends in the layer of 250–750 m in the WBS, AA, WSA, and CO regions indicate a strong heat discharge and an increasing outflow of heat from this layer; they are consistent with the heat content trends in the subsurface layers in the zone of 50–79°N of the World Ocean as a whole [21].

These tendencies in average annual values of T_w and Q are typical both of the warm and cold seasons. However, the higher correlations between these parameters are registered in the cold season, when convective processes intensify. This confirms the leading regime-forming role of winter processes for the analyzed regions [1, 17]. In this season, statistically significant correlations between variations in T_w and Q and the changes in the meridional or zonal components of wind speed are observed in the layer of 5–100 m in all regions ($R = |0.4–0.7|$). In the coastal region, these correlations are found not only in the cold intermediate layer, but also at deeper levels. The separate phases of variability in T_w and Q in the surface structural zone for each region are mainly consistent with each other (Figs. 3a and 3c). During the periods from the middle of the 1980s till the early 1990s and from the late 1990s till the early 2010s, abnormal heat loss and the cooling of the water column in the entire upper layer to 750 m occurred. This was associated with global trends in the World Ocean heat content resulting from the transformation of air pressure, wind, and ocean circulation fields [16, 21, 25]. The peculiarities of global changes in the subarctic Pacific are a display of heterogeneity and specificity of processes in different regions. In the southwestern part of the analyzed region, a strong source of heat to the atmosphere and advection to the neighboring ocean areas is the energy active zone of Kuroshio [11]. The analysis of GODAS data [15] showed that in the recent four decades, there have been positive trends towards an increase in the velocity and discharge of the main flow of Kuroshio in the upper 100-meter layer at the section between 33–34°N along 140°E, which are more pronounced in the cold season. At the same time, in neighboring water of the northern Philippine Sea, average annual SST steadily increased with a rate of 0.20–0.25 °C per decade, and positive trends in the speed of southern winds during the summer monsoon were registered. The phases of the increase and decrease in the current velocity are consistent with the variations in the anomalies of integral heat content in the layers of 5–100 and 100–250 m in the adjacent TZ and WSA regions. As noted above,

the stable accumulation of heat in the upper and intermediate layers takes place in these regions. The coefficients of correlation between the SST variations in the area of Kuroshio and in the WSA and TZ regions are statistically significant. The revealed changes in the water column and on the surface occur under the influence of atmospheric circulation on the system of currents [1]. For example, the pattern of trends in climate indices of the Pacific monsoon (PTW) and Pacific Decadal Oscillation (PDO) indicates the intensification of trade winds against a background of the PDO weakening in all seasons [13], which favors the intensification of Kuroshio and heat advection from the south to the neighboring areas in the southwestern subarctic region.

3.4. Correlation between Variability of Thermal Characteristics of Surface, Intermediate Layers and Climate Indices

The interannual trends in climate indices are mainly determined by the position, manifestation, and interaction of the main pressure centers being the seasonal atmospheric centers of action and depend on the chosen time period [9]. The peculiarities of atmospheric circulation over the study region in the autumn-winter season are determined by the interaction of two atmospheric centers of action: the Aleutian Low, that is formed over the ocean, and the Siberian High situated over the continent. In summer, the high-pressure zone (the North Pacific High) is formed over the ocean, and the low-pressure zone including the Asian and Far Eastern lows (which are usually united into one system) is activated over the continent [4]. The significant trend components were present in the interannual variations in climate indices [13]. The correlation with these components indicates the influence of different large-scale processes on the structure of pressure and wind fields and thermal conditions in the region [4]. The pattern of the corresponding relationships is expressed in the form of the spatial distribution of the coefficients of correlation between the climate indices and the fields of the anomalies of T_a , SST, and T_w at different horizons. The location and area of the regions where the separate circulation mechanisms affect the interannual variations in T_a and SST in different seasons, are consistent with each other, because the main features of the spatiotemporal structure of the principal EOF components of fluctuations in the anomalies of SST and T_a are identical. The coefficients of correlation of the separate climate indices and the atmospheric centers of action with SST for the distinguished areas and SST EOFs (C1–C3) in the warm (W) and cold (C) seasons are given below:

Index	PDO		NPI	SH – AL	PNA	AMO	AD
	W	C	C	C	C	C	W
Season	W	C	C	C	C	C	W
WBS	0.3	0.5	–0.2	–0.1	–0.1	0.2	0.2
AA	0.5	0.9	–0.3	0.3	0.3	0.0	0.3
WSA	–0.7	–0.5	0.5	–0.4	–0.4	0.5	–0.4
TZ	–0.7	–0.7	0.5	–0.4	–0.6	0.1	–0.5
ESA	0.3	0.4	–0.2	0.2	0.0	–0.3	0.4
CO	0.5	0.8	–0.5	0.4	0.5	0.2	0.3
C1	0.2	0.9	–0.5	0.4	0.5	–0.2	0.1
C2	–0.9	–0.1	0.2	–0.1	–0.5	–0.2	–0.6
C3	0.1	0.1	0.1	–0.1	0.0	0.5	–0.3

Here, SH – AL is the difference in the anomalies of surface air pressure between the Siberian High and the Aleutian Low; AD is surface pressure in the region of the Asian depression.

These data confirm the importance of the role of winter processes for most of the analyzed regions [1, 17], especially for the Alaskan-Aleutian and coastal ones, where statistically significant correlations between the variations in T_w and separate climate indices (PDO, NPI, SH – AL, and PNA) are observed to the depth of 500–750 m. In these areas, the zones of intensive convective mixing are located, whose depth in separate regions of the subarctic Pacific can exceed several hundred meters [1, 8]. Such estimates were also obtained during the analysis of data for the subarctic Atlantic [14]. In the coastal region in the cold season, the changes in T_w in all distinguished layers correlate with interannual variations both in the meridional and zonal components of wind speed ($R = |0.3–0.6|$). In some regions they correlate with the time factors of the first EOF mode of wind stress curl (AA, TZ, and CO), the second (WBS) and third (WSA, ESA, and CO) modes. The positive value of the trend in NPI indicates the weakening influence of the Aleutian Low on the circulation activity in the atmosphere in the cold season [13]. In the area of the western subarctic gyre [17], the moderate correlations ($R = 0.4–0.5$) between the variations in T_w and AMO are pronounced in the layer of 0–750 m in the cold season. In addition, the AMO fluctuations correlate with the time factors of the third SST EOF mode, as well as of the first and third EOF modes of wind stress curl

($R = -0.4 \dots -0.5$). Within the WSA region, there are areas with the maximum number of cyclones passing over the Northwest Pacific [4], as well as areas with the variability of wind stress curl corresponding to the first, the most energy-carrying EOF mode.

In the warm season, the correlations between the fields of SST, T_a , and AMO are observed only in the western subarctic region, and the correlations between SST and WP are pronounced in the north (WBS and AA regions). The effect of the variability in PDO and AD is manifested in the correlation with SST in most of the regions, but the PDO effect on T_w in the upper 100–200-meter layer is observed only in the WBS, AA, ESA, and CO regions. The change in the PDO phase and the AD deepening occurred in the study period, which indicates the accumulation of positive anomalies in the northern and western parts of the Pacific Ocean [4, 20]. The trend components and the correlation between the interannual variations in the climate index of the Hawaii High (Haw) and water temperature in the warm season are not pronounced. The trends in the Western Pacific climate index (WP) means its transition to the negative phase, which is associated with a decrease in the pressure gradient between the subtropical and subpolar latitudes, with the weakening of zonal atmospheric circulation in the middle troposphere at the level of 500 hPa, with the intensification of the inter-latitude exchange, and with the warming in the North Pacific sector [10].

4. CONCLUSIONS

The interannual variability of average annual SST in the subarctic Pacific is characterized by positive trends (on average 0.18 C/10 years), that are maximal in the west (0.2–0.4 C/10 years) and are minimal in the east of the study region (~0.1 C/10 years). In the warm season, the warming rate is about twice higher than in the cold season. In the northwestern and southwestern parts, where the zone of active cyclogenesis has been situated in the recent decades, the contribution of the trend to total variance of average annual SST makes up about 30–40%. The phase of accumulation of positive SST anomalies is pronounced after 2003 in the western part of the subarctic region and only since 2013 in the eastern part. Under general warming trends in 1982 to 2018, the average annual values of SST increased by 0.4–1.1 C in different parts of the subarctic region and by 0.7 C in the whole region.

The variations in water temperature T_w and the anomalies of heat content Q in the water column in different areas of the ocean are extremely uneven. In the southwestern subarctic region within the upper 750-meter layer, the positive trends in T_w and Q were observed in the warm and cold seasons in all analyzed layers of the water column; the general increase in average annual water temperature during 1980–2018 amounted to about 0.2–0.4 C. In the north and east, the negative trends in T_w and Q dominated in different layers of the water column; the general water temperature decrease was equal to 0.2–0.3 C, which indicates the intensification of the heat outflow and corresponds to the heat content trends in the subsurface layers of the zone of 50–79 N of the World Ocean as a whole. In the southeastern part of the subarctic region, the differently directed trends in T_w were observed in the analyzed period in the upper (to 250 m) and lower (250–750 m) layers of the water column. During the cold season, when convective processes intensify, statistically significant correlations between T_w and Q and changes in the meridional or zonal components of wind speed ($R = |0.4-0.7|$) are manifested in the upper 100-meter layer in all regions.

The phases of alternating warm and cold periods are consistent with the trends in the characteristics of the atmospheric centers of action, climate indices, and various climatic parameters.

FUNDING

The research was performed in the framework of the Governmental Assignment of Il'ichev Pacific Oceanological Institute (Far Eastern Branch of Russian Academy of Sciences), theme 0271-2019-0003 (state registration number AAAA-A17-117030110042-2).

REFERENCES

1. V. I. Byshev, A. L. Figurkin, and I. M. Anisimov, "Modern Climate Change in Thermohaline Structure of North Pacific Water," *Izv. TINRO*, No. 185 (2016) [in Russian].
2. *Second Roshydromet Assessment Report on Climate Change and Its Consequences in the Russian Federation*, Ed. by V. M. Kattsov and S. M. Semenov (Roshydromet, Moscow, 2014) [in Russian].
3. A. N. Gezentsvei, "Divergence of Drift Flows and Heat Transfer by Currents in the North Pacific and North Atlantic," *Trudy IO AN SSSR*, **9** (1954) [in Russian].
4. S. Yu. Glebova, "Cyclones over the Pacific Ocean and Far Eastern Seas in Cold and Warm Seasons and Their Influence on Wind and Thermal Regime in the Recent Two Decades," *Izv. TINRO*, No. 193 (2018) [in Russian].

5. G. V. Gruza, E. Ya. Ran'kova, E. V. Rocheva, and V. D. Smirnov, "Geographic and Seasonal Features of Modern Global Warming," *Fundamental'naya i Prikladnaya Klimatologiya*, No. 2 (2015) [in Russian].
6. V. V. Efimov and A. E. Anisimov, "Climatic Parameters of Wind-field Variability in the Black Sea Region: Numerical Reanalysis of Regional Atmospheric Circulation," *Izv. Akad. Nauk, Fiz. Atmos. Okeana*, No. 3, **47** (2011) [*Izv., Atmos. Oceanic Phys.*, No. 3, **47** (2011)].
7. V. A. Luchin and V. I. Matveev, "Interannual Variability of Thermal State of Cold Subsurface Layer in the Sea of Okhotsk," *Izv. TINRO*, No. 187 (2016).
8. A. M. Muromtsev, E. V. Borisov, and V. M. Gruzinov, "Thermal Processes in the Upper Ocean Layer in the Area of Kuroshio," *Trudy GOIN*, No. 100 (1970) [in Russian].
9. G. N. Panin, T. Yu. Vyruchalkina, and I. V. Solomonova, "Regional Climate Change in the Northern Hemisphere and Its Interrelation to Circulation Indices," *Problemy Ekologicheskogo Monitoringa i Modelirovaniya Ekosistem*, No. 23 (2010) [in Russian].
10. V. V. Popova and A. B. Shmakin, "Regional Structure of Surface-air Temperature Fluctuations in Northern Eurasia in the Latter Half of the 20th and Early 21st Centuries," *Izv. Akad. Nauk, Fiz. Atmos. Okeana*, No. 2, **46** (2010) [*Izv., Atmos. Oceanic Phys.*, No. 2, **46** (2010)].
11. A. E. Rozhdestvenskii and G. A. Malyshev, "Evaluation of Sources and Sinks of Heat in the Northern Hemisphere Atmosphere," *Uchenye Zapiski Rossiiskogo Gosudarstvennogo Gidrometeorologicheskogo Universiteta. Meteorologiya*, No. 45 (2016) [in Russian].
12. I. D. Rostov, E. V. Dmitrieva, N. I. Rudykh, and A. A. Vorontsov, "Climatic Changes in Thermal Conditions in the Kara Sea over the Recent 40 Years," *Problemy Arktiki i Antarktiki*, No. 2, **7** (2019) [in Russian].
13. I. D. Rostov, E. V. Dmitrieva, N. I. Rudykh, and A. A. Vorontsov, "Climatic Changes in Thermal Conditions of Marginal Seas in the Western Pacific," *Meteorol. Hidrol.*, No. 3 (2020) [Russ. Meteorol. Hydrol., No. 3, **45** (2020)].
14. A. S. Falina, A. A. Sarafanov, S. A. Dobrolyubov, V. S. Zapotyl'ko, and S. V. Gladyshev, "Convection and Stratification of Water in the North Atlantic as Derived from Measurements in Winter of 2013/14," *Vestnik Moskovskogo Universiteta. Ser. 5. Geografiya*, No. 4 (2017).
15. D. W. Behringer and Y. Xue, "Evaluation of the Global Ocean Data Assimilation System at NCEP: The Pacific Ocean," in *Eighth Symposium on Integrated Observing and Assimilation Systems for Atmosphere, Oceans, and Land Surface, AMS 84th Annual Meeting* (Washington State Convention and Trade Center, Seattle, Washington, 2004).
16. M. H. England, S. McGregor, P. Spence, G. A. Meehl, A. Timmermann, W. Cai, A. Sen Gupta, M. J. McPhaden, A. Purich, and A. Santoso, "Recent Intensification of Wind-driven Circulation in the Pacific and the Ongoing Warming Hiatus," *Nature Climate Change*, No. 3, **4** (2014).
17. F. Favorite, A. J. Dodimead, and R. Nasu, "Oceanography of the Subarctic Pacific Region," *Bulletin No. 33 of Intern. North Pacific Fisheries Commission* (Vancouver, Canada, 1976).
18. *IPCC, 2013: Climate Change 2013: The Physical Science Basis. Contribution of Working Group I to the Fifth Assessment Report of the Intergovernmental Panel on Climate Change*, Ed. by T. F. Stocker, D. Qin, G.-K. Plattner, M. Tignor, S. K. Allen, J. Boschung, A. Nauels, Y. Xia, V. Bex, and P. M. Midgley (Cambridge University Press, Cambridge, United Kingdom and New York, NY, USA, 2013).
19. E. Kalnay, M. Kanamitsu, R. Kistler, W. Collins, D. Deaven, L. Gandin, M. Iredell, S. Saha, G. White, J. Woolen, Y. Zhu, M. Chelliah, W. Ebisuzaki, W. Higgins, J. Janowiak, K. C. Mo, C. Ropelewski, J. Wang, A. Leetmaa, R. Reynolds, R. Jenne, and D. Joseph, "The NCEP/NCAR 40-year Reanalysis Project," *Bull. Amer. Meteorol. Soc.*, **77** (1996).
20. M. Latif and T. P. Barnett, "Causes of Decadal Climate Variability over the North Pacific and North America," *Science*, **266** (1994).
21. S. Levitus, J. Antonov, and T. Boyer, "Warming of the World Ocean, 1955–2003," *Geophys. Res. Lett.*, **32** (2005).
22. V. Luchin, A. Kruts, O. Sokolov, et al., *Climatic Atlas of the North Pacific Seas 2009: Bering Sea, Sea of Okhotsk, and Sea of Japan (NOAA Atlas NESDIS 67V)*, Ed. by V. Akulichev, Yu. Volkov, V. Sapozhnikov, and S. Levitus (U.S. Gov. Printing Office, Washington, DC, 2009).
23. R. W. Reynolds, N. A. Rayner, T. M. Smith, D. C. Stokes, and W. Wang, "An Improved in Situ and Satellite SST Analysis for Climate," *J. Climate*, No. 13, **15** (2002).
24. D. Seidov, O. K. Baranova, T. P. Boyer, A. V. Mishonov, and A. R. Parsons, *Northern North Pacific Regional Climatology, Regional Climatology Team* (NOAA/NCEI, 2017), www.nodc.noaa.gov/OC5/regional_climate/nnplclimate.
25. K. E. Trenberth and J. T. Fasullo, "An Apparent Hiatus in Global Warming?," *Earth's Future*, No. 1, **1** (2013).
26. M. Uda, "Oceanography of the Subarctic Pacific Ocean," *J. Fish. Res. Board of Canada*, No. 1, **20** (1963).
27. *WMO Provisional Statement on the State of the Global Climate in 2019* (WMO, 2019), <https://public.wmo.int/en/our-mandate/climate/wmo-statement-state-of-global-climate>.
28. C. Wu, Y. Lin, Y. Wang, N. Keenlyside, and J. Yu, "An Atlantic-driven Rapid Circulation Change in the North Pacific Ocean during the Late 1990s," *Scientific Reports*, No. 9 (2019).